ELSEVIER

Chemical Engineering Journal 71 (1998) 1–9

Chemical Engineering Journal

Simulation of flow hydrodynamics in a pulsed solvent extraction column under turbulent regimes

G. Angelov[a,*], C. Gourdon[b], A. Liné[c]

[a] *Institute of Chemical Engineering, Bulgarian Academy of Sciences, Acad. G. Bonchev Str-B1.103 1113, Sofia, Bulgaria*
[b] *Ecole Nationale Supérieure des Ingénieurs de Génie Chimique, Toulouse, France*
[c] *Institut National des Sciences Appliquées, Toulouse, France*

Received 24 October 1995; received in revised form 9 February 1997; accepted 3 June 1998

Abstract

Mathematical description and numerical simulation of the flow hydrodynamics is carried out for the case of a pulsed turbulent flow in extraction columns with internals of alternating discs and rings (DRC). In this work, the flow hydrodynamics (flow structure, velocity fields, flow energy parameters etc.) are studied related to the geometrical parameters of the internals and to pulsation intensity. It is found that the flow pattern of a DRC is characterized by the presence of permanent large vortices as well as by permanent zones of low and high levels of the turbulent kinetic energy. The latter is responsible for the drop break-up processes and for interphase surface formation. A simple dependence of the turbulent energy parameters (turbulent kinetic energy k and its dissipation rate ε) on the pulsation intensity is estimated. The influence of the internals design on the stage energy level is characterized by constants independent on the pulsation intensity. The results are also used to create a data bank of local values of velocity, pressure, turbulent kinetic energy and its dissipation rate under various stage geometry parameters and various intensities of the pulsation applied to the flow. The contents of this data bank are useful for development of correlations for prediction of important process parameters used in apparatus design and scale-up.

Keywords: Hydrodynamics; Extraction column; Turbulent flow; Flow structure

1. Introduction

Pulsed columns with internals of immobile discs and rings (DRC) have been extensively studied for a wide range of liquid–liquid [1–4] and solid–liquid [5–7] extraction applications. Attractive results were obtained concerning overall mass transfer characteristics and operational performance which motivated various industrial application [4]. Nevertheless, the industrial apparatuses are designed in a rather empirical way because of lack of information on some basic processes in such type of equipment. Among them, the mechanisms of interphase surface formation play a key role as they define the area for interfacial interactions (mass transfer, chemical reactions etc.). Generally, the droplet break-up processes in a contact apparatus are controlled by the energy of the main flow (its own energy and additionally supplied external energy) and by the flow structure. Other parameters, such as pressure drop and axial mixing, also depend on the flow structure specified by the operational regime and the internals design. Consequently, the aim of this work is to study the flow hydrodynamics (flow structure, velocity fields, flow energy parameters etc.) related to the geometrical parameters of the internals and to pulsation intensity, as far as it is relevant to the further prediction of important process characteristics.

2. Column geometry parameters

A sketch for a DRC is given in Fig. 1.

The stage geometry is defined by two parameters: (a) the distance between a disc and a ring H or by the ratio, h=H/D_c. (b) the voidage (plate open free area) F is defined as

$$F = \frac{D_r^2}{D_c^2} = \frac{R_r^2}{R_c^2} = \frac{(D_c^2 - D_d^2)}{D_c^2}$$

where D_r (R_r) is diameter (radius) of the ring aperture, D_c (R_c) the column diameter (radius) and D_d the disc diameter.

*Corresponding author.

1385-8947/98/$ – see front matter
PII: S1385-8947(98)00111-9

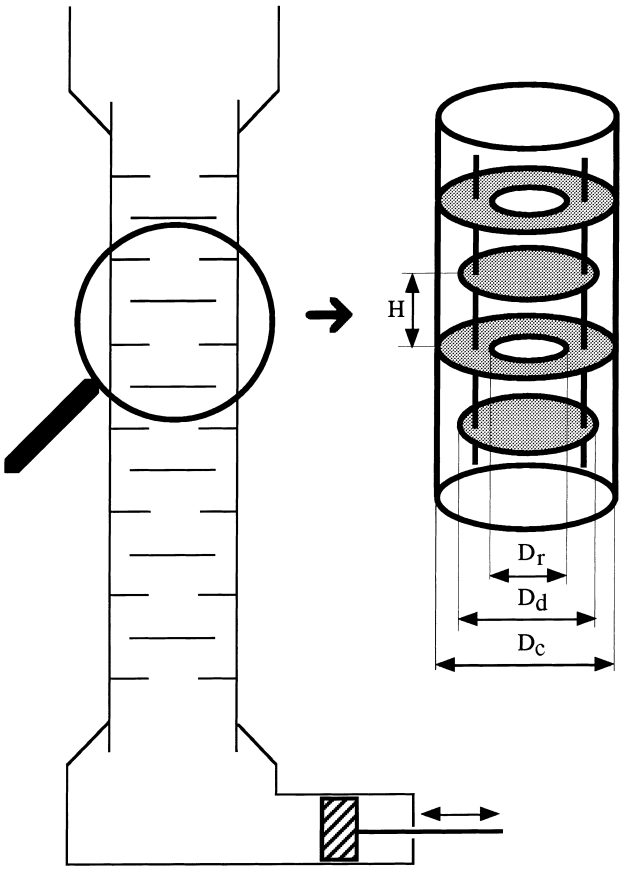

Fig. 1. Sketch of a DRC.

The range of variation of the stage geometry parameters is chosen by practical considerations and by industrial experience: disc diameter D_d should be larger than ring aperture diameter D_r in order to avoid an undesired direct axial flow through the column. The case of equal diameters ($D_d = D_r$) corresponds to a voidage $F = 0.5$. Thus the cases F>0.5 have no practical interest. The case $F = 1$ corresponds to a column without internals (hollow tube). A small distance between the plates will induce a larger pressure drop and a greater energy consumption. On the other side, a large interplate distance (more than the column diameter) will result in a reduced efficiency.

The selection of intervals that define a reasonable range of geometric parameters to be studied is given below: $F = 0.2$–0.5, h=0.1–0.4

Four values of h and two values of F are considered here ($h1 = 0.086$, $h2 = 0.155$, $h3 = 0.31$, $h4 = 0.38$, $F1 = 0.23$, $F2 = 0.43$). The combination of these values results in eight different stage geometries noted as $h1F1$; $h1F2$; $h2F1$; $h2F2$; H3$F1$; $h3F2$; $h4F1$; $h4F2$. The geometry $h2F1$ corresponds to a pilot-plant column with experimental data available. In this particular case the stage dimensions are: column diameter $D_C = 0.29$ m; stage height -0.09 m; distance between a disc and a ring H=0.045 m; disc diameter $D_d = 0.253$ mm; diameter of the ring aperture $D_r = 0.14$ m.

3. Flow dynamic parameters

In order to make a mathematical description of the hydrodynamics in the column under study, the flow was assumed to be single phase two-dimensional axisymmetrical flow of an incompressible Newtonian liquid. The basic equations used were Reynolds equations associated with the k–ε turbulence model [8,9].

Additionally, a sinusoidal periodic pulsation is superimposed in order to simulate the pulsed flow in the column

$$U(t) = \pi A f \cos(2\pi f t) \tag{1}$$

where $U(t)$ is the superficial velocity of the pulsed flow at the instant t; A and f are pulsation's peak-to-zero amplitude and frequency.

The mean superficial velocity during a pulsation cycle is

$$V_s = \frac{1}{T}\int_0^T |U(t)|\mathrm{d}t \tag{2}$$

where T is the period of pulsation.

The solution of Eqs. (1) and (2) leads to

$$V_s = 2Af \tag{3}$$

and Re number is defined as

$$\mathrm{Re} = \frac{V_s D_c}{\nu} = \frac{2AfD_c}{\nu} \tag{4}$$

with ν being the kinematic viscosity.

The column is considered to be built of identical stages. Thus, a single stage modeling of a single phase flow is expected to be representative of the hydrodynamic situation in the main active part of the column.

4. Boundary conditions

The boundary conditions at solid walls are specified at a grid point outside the viscous sublayer and not right at the wall. In this region a logarithmic law of the wall is used

$$\frac{U(\delta)}{U^*} = \frac{1}{\kappa}\ln(E\delta^+) \tag{5}$$

where U^* is the friction velocity, $\delta^+ = \delta U^*/\nu$, κ the von Karman constant, E a roughness scaling parameter equal to nine for smooth walls.

The assumption of local equilibrium together with the logarithmic law results in

$$k(\delta) = \frac{U^{*2}}{C_\mu^{1/2}} \tag{6}$$

$$\varepsilon(\delta) = \frac{U^{*3}}{\kappa\delta} \tag{7}$$

C_μ is a constant of the k–ε model with standard value 0.09 [9].

The boundary conditions at the stage open limits are known and well defined for the case $h2F1$ which corresponds to the existing column geometry and experimental measurements are available. Meanwhile, it was estimated [10] that at higher Re numbers the applied software ARMOR [11] gives solutions insensitive to moderate variations of the boundary conditions. Similar observations were made in the considered case of pulsed quasi-stationary flow regime [12]. Thus it is not absolutely necessary to use very precise data as boundary conditions. An uniform flat entry profile of the axial velocity V_z was applied at the entrance/exit zones, calculated by Eq. (1) for various Re numbers with respect of the free open area of the ring. The input radial velocity V_r was assumed to be zero for all configurations as indicated by the experimental measurements for the configuration $h2F1$ [12–14]. For this configuration mean values based on experimental measurements of k at the stage entrance [13] were used. The respective values of the turbulent energy dissipation rate ε were obtained by the model relation:

$$\varepsilon = \frac{C_\mu k^2}{\nu_t} \tag{8}$$

An approximate value of turbulent viscosity $V_t = 100\nu$ was assumed to be reasonable for determination of the initial and boundary conditions. This choice will be justified later.

For stage configurations other than $h2F1$, the approximate boundary values of k and ε at the open boundaries were estimated by use of simple relations [12], validated for the interval of Re 5000–15 000:

$$\ln(k/V_s^2) = -5.24\text{-}4.53 \ln F \tag{9}$$

The boundary conditions for ε were introduced according to the relation

$$\varepsilon = \frac{2}{hD_c} k^{3/2} \tag{10}$$

which reflects the influence of the inter-stage distance. Eq. (10) follows from the model equation

$$\varepsilon \approx \frac{k^{3/2}}{L} \tag{11}$$

and from the estimation [10,13] for turbulent macroscale in a DRC

$$L \approx \frac{H}{2} \tag{12}$$

5. Results and discussion

The results presented below were obtained within the range of Re numbers 5000–15 000. Four values of Re were systematically used, namely 5000, 8700, 10 000, and 15 000. Calculations for other values from the same range were also made in order of comparison with particular experimental data. The same range has been studied experimentally by Oh [13] who has not registered significant separate influence of the amplitude and frequency of pulsation on the turbulent flow parameters, i.e. their influence is translated by their product, respectively, by Re number.

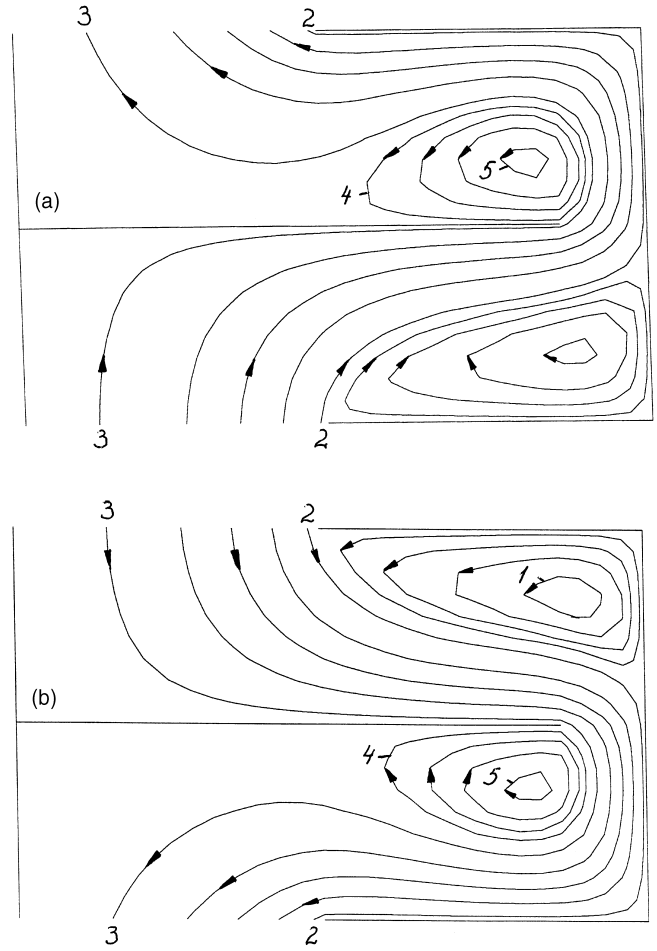

Fig. 2. Stream lines pattern for Re = 10 000 stage geometry case $h2F1$ (a) admission phase $t/T = 0.5$; the corresponding values of the stream line function are: (1) -4, 1×10^{-3}; (2) -3, 3×10^{-3}; (3) -2, 1×10^{-4}; (4) 1, 0×10^{-4}; (5) 8, 9×10^{-4}. (b) Escape phase $t/T = 0.35$; (1) 2, 5×10^{-3}; (2) 2, 0×10^{-3}; (3) 2, 0×10^{-4}; (4) -1, 0×10^{-4}; (5) -5, 4×10^{-4}.

Local values of the mean velocity, turbulent kinetic energy k and its dissipation rate ε inside the stage were obtained by numerical simulations of pulsed flows in DRC with various stage geometry. Further, the velocity vectors and stream lines were drawn and the flow pattern was graphically visualized as well as the energy distribution inside the stage. A typical stream line pattern is illustrated on Fig. 2. It is characterized by the presence of two large vortices – one in the lower part and another in the upper part of the compartment.

During the admission phase (ascending flow – Fig. 2(a)) the vortex in the lower part of the compartment is placed near the stage corner. It was found that it did not change its volume and position but it changed its intensity proportion-

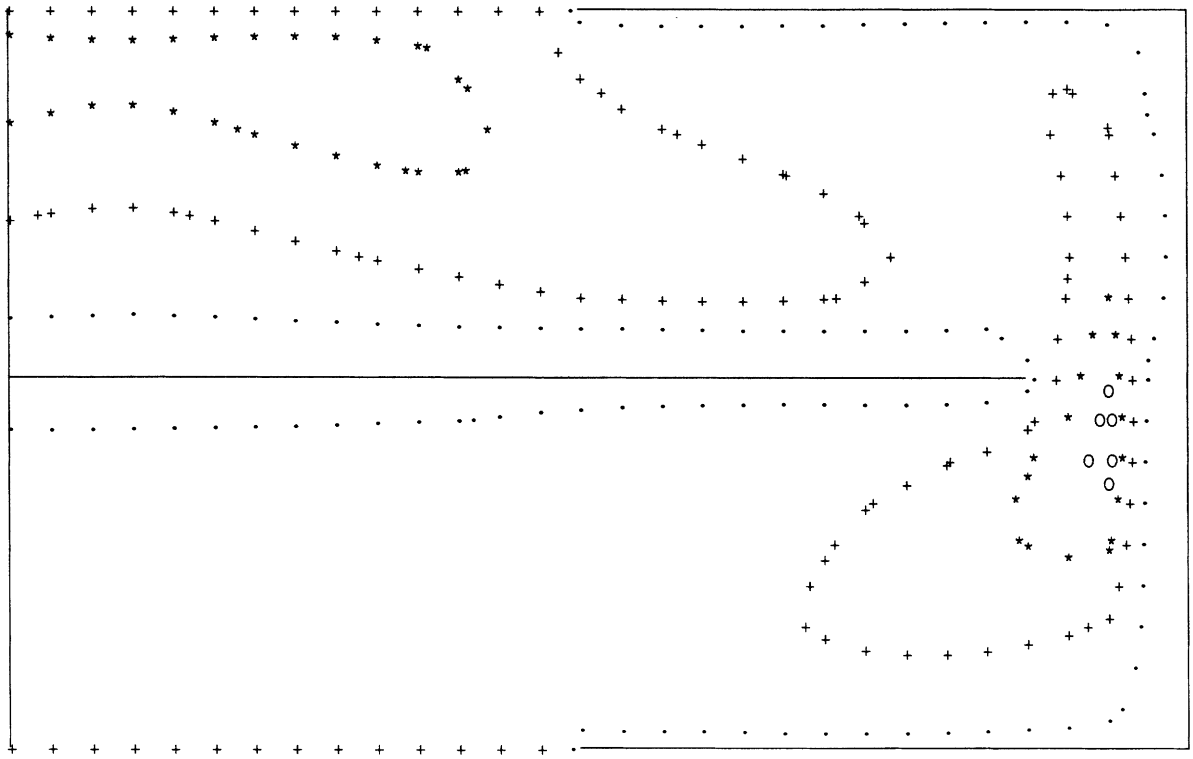

Fig. 3. Turbulent kinetic energy field during the admission phase $t/T = 0.05$; case $h2F1$; Re = 10 000. The corresponding levels of the isokinetic lines (m^2/s^2) are: (····) −0.0010; (++++) −0.0043; (****) −0.0070; (oooo) −0.0095.

ally to the flow velocity. During the escape phase (descending flow – Fig. 2(b)) the vortex zone is located under the disc and near to its edge with the same direction of rotation but occupying a smaller volume. The visual behavior of the vortex is like that of an oscillating pulsed zone.

The flow pattern in the compartment upper part is the same but shifted at a half period.

The flow structure is not significantly affected by the increase of Re number. Slight changes of the volume of permanent vortices are observed. The intensity of circulation follows the increasing of Re number.

Experimental observations on two phase pulsed flow in an extractor with the same geometry [1] have proved the existence of permanent vortices with behavior described above. Permanent vortices are also reported in other simulation studies on this type of columns [15,16].

In addition to the laminar case [15], the turbulent flow modeling supplies important information on the energy distribution at the stage, which directly affects the drop break-up phenomena. Turbulent kinetic energy iso-levels during the admission phase are shown in Fig. 3.

The energy is concentrated in the annular aperture between the disc and column wall and also in a median section between the disc and upper ring. During the escape phase the situation is symmetrical – the high energy level is located at the median section under the disc and lower ring and always in the gap between the disc and wall. This result implicitly agrees with the experimental observations on the drop behavior in a DRC. The same 'active zones' are found to be places of intensive break-up of drops [14].

The space distribution of ε is similar to that of k and will not be illustrated here.

The influence of pulsation intensity on the mean values (time and space averaged) of energy parameters k and ε for various stage geometry is shown on Figs. 4 and Fig. 5.

The evolution can be evidently presented in the general form

$$\langle k \rangle = K_k (Af)^2 \tag{13}$$

$$\langle \varepsilon \rangle = K_\varepsilon (Af)^3 \tag{14}$$

Keeping a constant pulsation intensity and following the evolution of k and ε, the qualitative influence of the stage geometry can be immediately seen. The higher is the plate distance (translated by the parameter h), the lower are the mean local values of kinetic energy k and its dissipation rate ε. The influence of plate open area F is similar. These results are logical and confirm that realistic pictures are obtained in the frames of this simulation.

Similar linear dependencies $k = f(Af)^2$ and $\varepsilon = f(Af)^3$ are detected in experimental observations on DRC [13,14]. Obviously, the constants K_k and K_ε which represent line slopes on Figs. 4 and 5, depend on the stage geometry and do not depend on the pulsation intensity, since (Af) is the unique scaling velocity. K_k is dimensionless as the dimension of k (m^2/s^2) is consistent with the dimension of

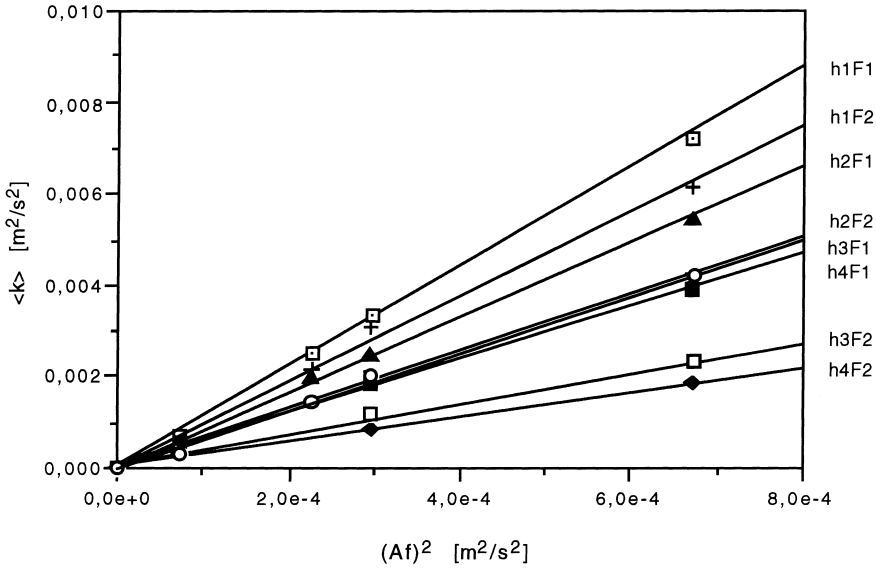

Fig. 4. Turbulent kinetic energy vs. pulsation intensity.

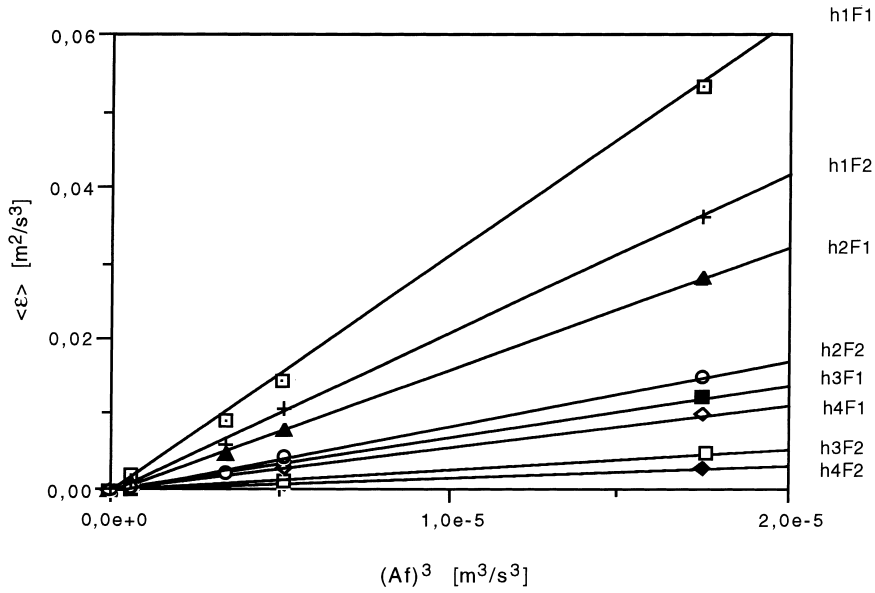

Fig. 5. Dissipation of the turbulent kinetic energy vs. pulsation intensity.

the argument $(Af)^2.K_\varepsilon$ has a dimension 1/1 where 1 is a size parameter. Its physical meaning can be found considering the approximation (11) derived from the k–ε model.

Introducing in (11) $\langle k \rangle$ and $\langle \varepsilon \rangle$ from Eqs. (13) and (14) it follows

$$K_\varepsilon \approx \frac{K_k^{3/2}}{L} \tag{15}$$

It is seen that the size parameter included in K_ε can be interpreted as the turbulent macroscale.

The values of the turbulent macroscale L can be obtained from calculated values of k and ε. Fig. 6 shows the diagram of iso-values of L in a stage with interplate distance $H = 0.045$ m. Most part of these values are sized between 0.02 and 0.03 m. The values of L for a smaller interplate distance $H = 0.025$ m were found to be sized between 0.01 and 0.015 m. Generally, the order of magnitude of the turbulent macroscale appears to be about half of the interplate distance. This result confirms once more the reliability of the estimation (12).

The values of the ratio turbulent viscosity/molecular viscosity ν_t/ν were found to be in the range 10–180 for Re = 5000; 10–220 for Re = 10 000 and up to 300 for Re = 15 000. The last case is illustrated in Fig. 7 and represents a typical distribution of this quantity on the stage.

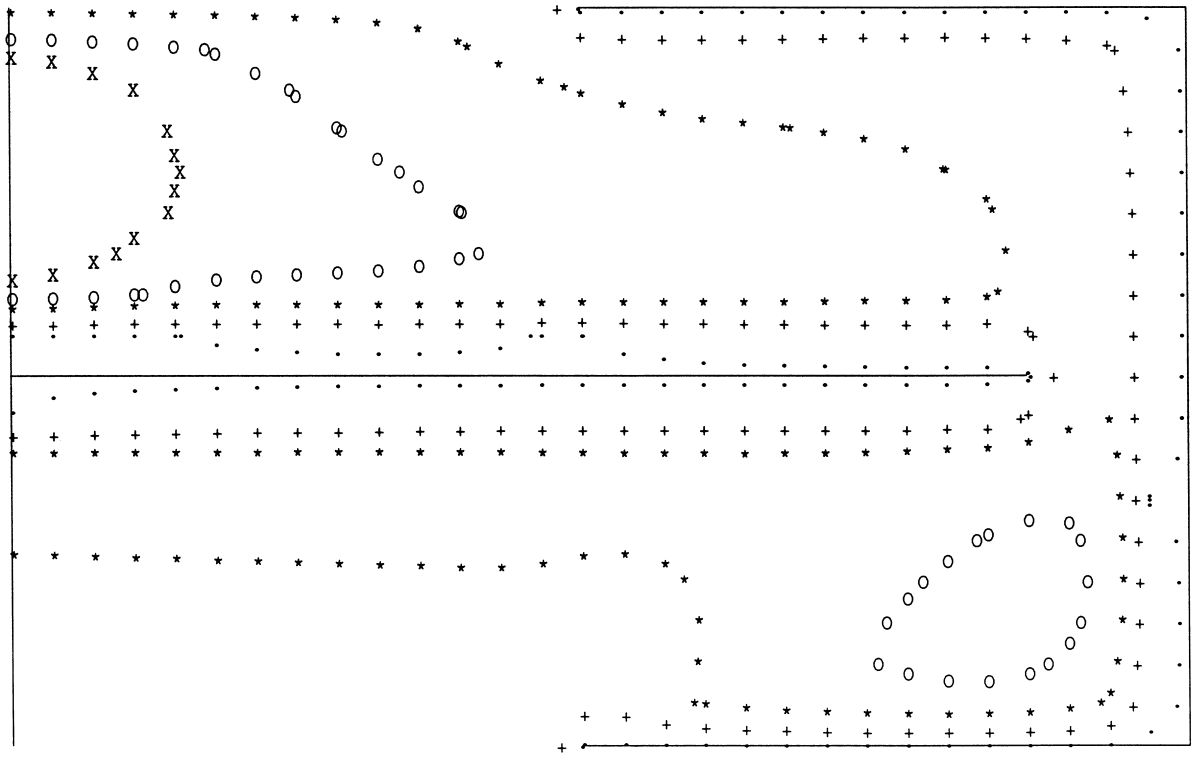

Fig. 6. Iso-values of turbulent macroscale L in the stage. Case *h*2*F*1; Re = 10 000; admission phase $t/T = 0.05$; distance between the disc and ring $H = 0.045$ m. (····) −L = 0.0015 m; (++++) −L = 0.01 m; (∗∗∗∗) −L = 0, 02 m; (○○○○) −L = 0.03 ; (xxxx) −L = 0.035 m.

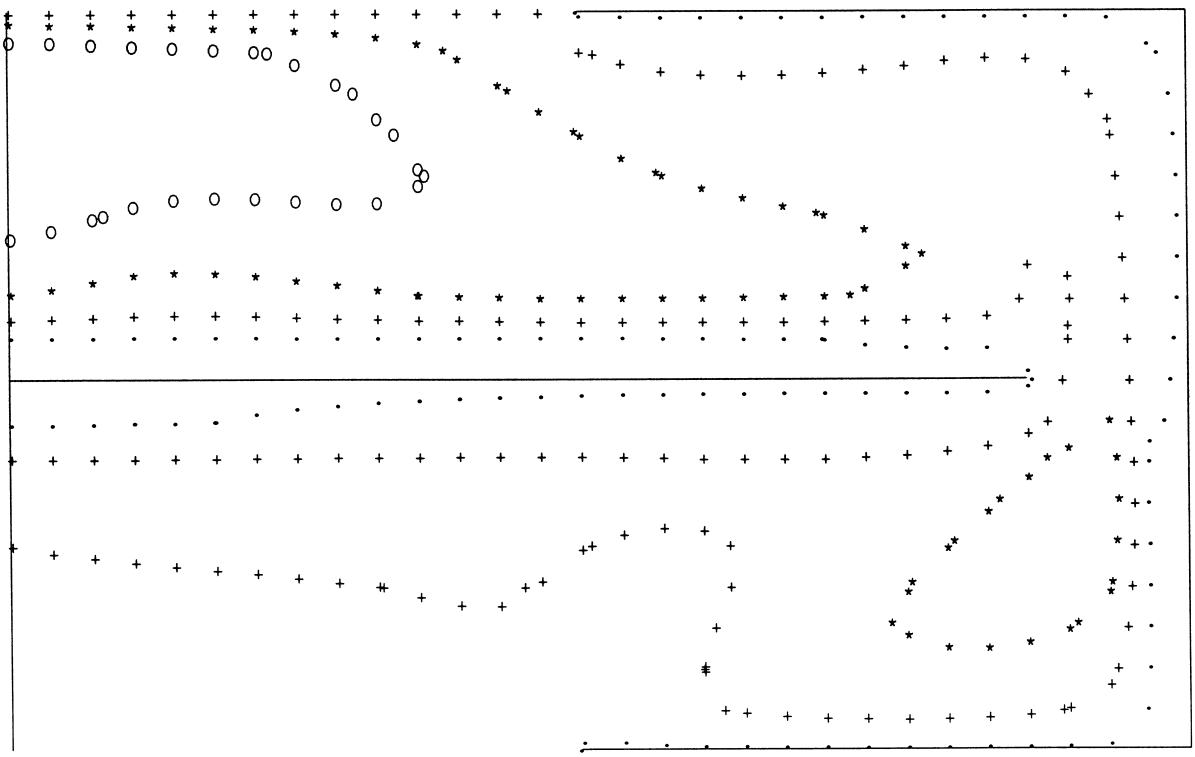

Fig. 7. Iso-values of the ratio turbulent viscosity/molecular viscosity ν_t/ν; Case *h*2*F*1; Re = 15 000, admission phase $t/T = 0.05$; $H = 0.045$ m. (····) $-\nu_t/\nu = 10$ (++++) $\nu_t/\nu = 100$; (∗∗∗∗) $\nu_t/\nu = 200$; (○○○○) $\nu_t/\nu = 300$.

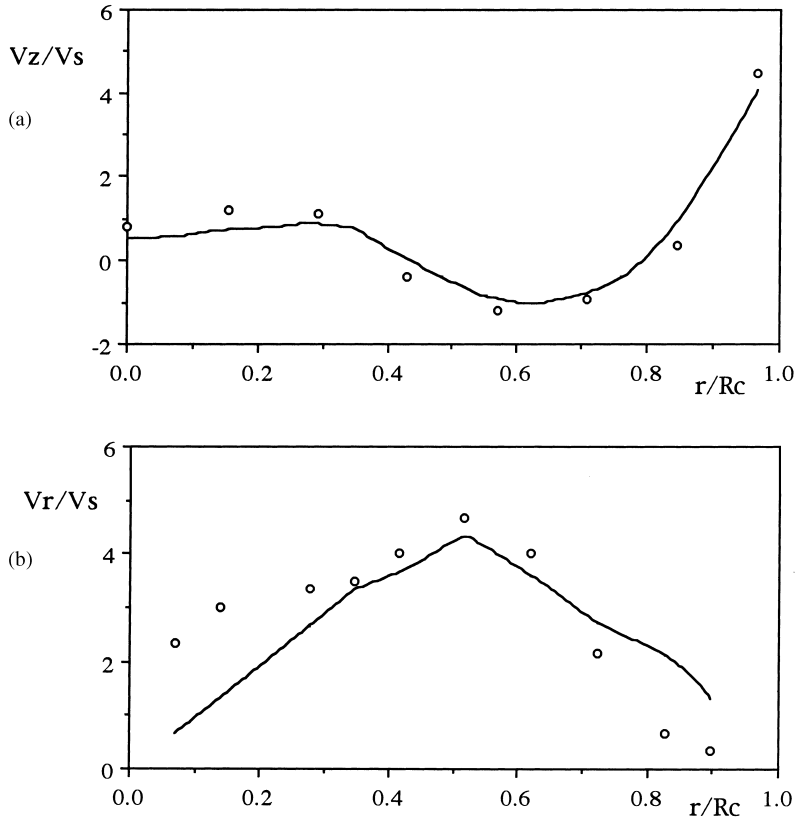

Fig. 8. Velocity profiles in the median cross-section. ○ –experimental values; ———— simulated profile. (a) Axial velocity in a permanent flow; Re = 6000 (b) Radial velocity in a pulsed flow, $t/T = 0{,}4$, Re = 8700.

This result is to support the choice of the value of $\nu_t = 100\nu$ used in the initial and boundary conditions. On the other hand, Fig. 7 shows that the turbulent viscosity is not uniformly distributed in the stage. Lower values are located near the rigid walls and larger values are located in the zones of higher energy level.

The simulation results can be compared with experimental data for the particular case of the existing pilot column 0.29 m in diameter, 0.045 m interplate distance, and plate free area $F = 0.23$. A direct comparison is possible between the measured and calculated local velocities. Fig. 8 illustrates some velocity profiles for various Re numbers in the median cross-section equidistant from the disc and ring. The fitting is better in case of permanent flow. A possible reason lies in the simplicity and higher precision of the measuring procedure in the case of permanent flow. The sophisticated measurements in pulsed flow could involve personal errors that make the experimental results less reliable.

Fig. 9 represents the simulated time-average distribution of the turbulent kinetic energy k at the median cross-section, compared to the experimental results [13]. A satisfying agreement is seen, the discrepancy between simulation and experiment becoming smaller for larger Re numbers.

A further indirect comparison with experimental results can be searched at the level of the process of drop breakage which is controlled by the flow energy. Laulan [14] has studied the drop break-up phenomena and has reported experimental data for the maximal stable drop diameter $d_{\max}$ in a DRC. $d_{\max}$ is related to the turbulent kinetic energy through the relation:

$$\mathrm{We_c} = \frac{\rho_c k d_{\max}}{\sigma} \tag{16}$$

where $\mathrm{We_c}$ is the critical Weber number.

For the particular operating conditions and the considered stage geometry $\mathrm{We_c} = 0.26$ (see Appendix A).

The local values of k obtained by simulation were selected over the energy containing 'active zones' to calculate mean k-values $\langle k \rangle_a$. Plotted vs. the pulsation intensity, it is obtained

$$\langle k \rangle_a = 12.5(Af)^2 \tag{17}$$

$\mathrm{d_{max}}$ can be calculated from the expression (17) involved in (16). The results are compared with experimental data in Table 1. It is seen that at lower Re the discrepancy is greater, but for more intensive turbulent regimes of practical interest the correlation (17) better fits the experimental data. Although this comparison is for a particular case, similarity considerations could enhance the applicability of numerical results.

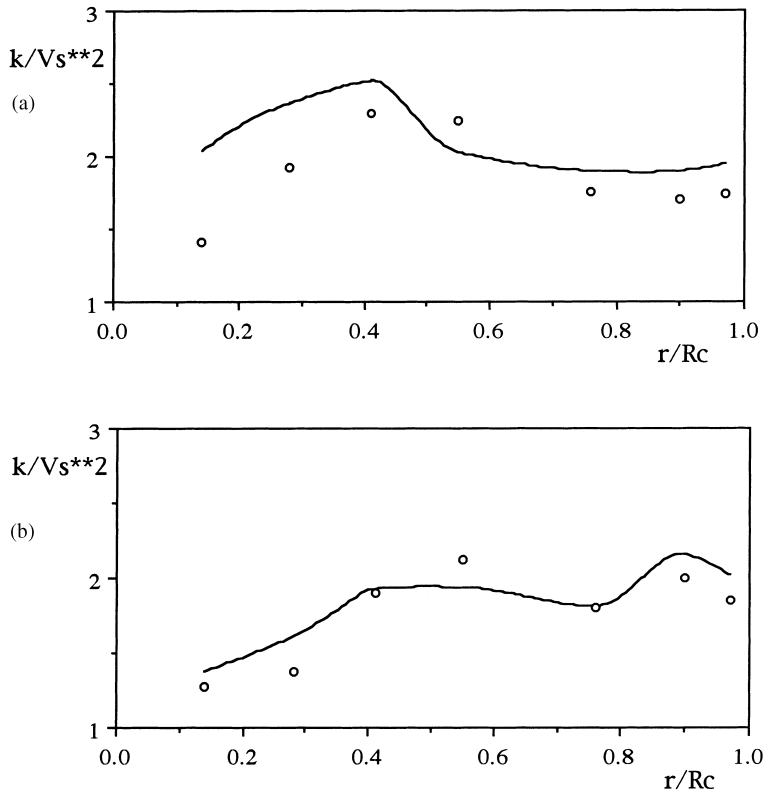

Fig. 9. Turbulent kinetic energy (time-averaged over a pulsation period) in the median cross-section. ○ – experimental results; ———— simulated profile (a) Re = 10 000; (b) Re = 15 000.

Table 1

Re	Af (cm s^{-1})	d_{max} (mm)	
		Experimental	Correlation (Eq. (17))
7200	1.2	3.8	4.3
9000	1.5	2.5	2.8
10 800	1.8	2.0	2.0

6. Conclusions

Computer simulation of the hydrodynamics of a column with internals of discs and rings is carried out based on the mathematical description using quasi-steady energy - dissipation turbulence model (k–ε). Pulsed flow under turbulent regimes is studied. Data about local values of the flow velocity, stream lines, and energy distribution on the stage are obtained for high Re numbers and for various stage geometry. They are to be used for development of correlations determining the energy parameters k and ε as a function of the stage configuration and pulsation intensity.

The evolution of flow structure during the pulsation period is described. The information for space distribution of turbulent energy parameters is used to estimate the macroscale of turbulence in the stage of such kind of equipment and to localize the regions of high level of turbulence – 'active zones' where intensive drop break-up is experimentally observed.

The study on pulsation intensity influence on the energy parameters mean values manifests simple linear dependencies for all used combinations of plate geometry parameters. The results obtained are consistent with observations on experimental pilot columns with internals of discs and rings and conform to the presumptions of the theory of turbulence as well.

Acknowledgements

The partial financial support of CNRS – France, Bulgarian Academy of Sciences and Bulgarian Fund for Scientific Research is gratefully acknowledged.

Appendix A

Calculation of maximum stable drop diameter

Particle Weber number is defined as a ratio of the kinetic and drop surface energy:

$$\mathrm{We} = \frac{\rho_c u'^2 d^3}{\sigma d^2} = \frac{\rho_c u'^2 d}{\sigma} \tag{A.1}$$

where d is the drop diameter, σ the interfacial tension, ρ_c the continuous phase density and u' the RMS (root mean square) of velocity fluctuations.

It is known [17] that

$$k = c_1 u'^2 = c_2(\varepsilon \mathrm{L})^{2/3} \tag{A.2}$$

and Eq. (A.1) takes the form

$$\mathrm{We} = \frac{\rho_c k d}{\sigma} = \frac{\rho_c (\varepsilon L)^{2/3} d}{\sigma} \tag{A.3}$$

where L is the turbulent macroscale and c_1, c_2 the constants.

When the dynamic pressure forces prevail over the surface forces, the drop will break. Thus, it exists a value of We corresponding to the equilibrium ratio between the maximum stable drop diameter d_{max} and the dynamic pressure forces. Currently d_{max} has the same order of magnitude as the turbulent macroscale L and Eq. (A.3) becomes

$$\mathrm{We}_c = \frac{\rho_c k d_{max}}{\sigma} = \frac{\rho_c \varepsilon^{2/3} d_{max}^{5/3}}{\sigma} \tag{A.4}$$

We_c can also be described in terms of the surface energy level of the mother and daughter drops [18,19]

$$\mathrm{We}_c = \frac{\Delta E_s}{\pi d^2 \sigma} \tag{A.5}$$

Considering a mother drop breaking into n equal daughter drops, the difference in the surface energy of mother and daughter drops $\Delta \mathrm{E}_s$ is

$$\Delta E_s = n\pi \left[\left(\frac{d}{n} \right)^{1/3} \right]^2 \sigma - \pi d^2 \sigma = \pi d^2 \sigma (n^{1/3} - 1) \tag{A.6}$$

and

$$\mathrm{We}_c = n^{1/3} - 1 \tag{A.7}$$

Laulan [14] has reported results on measurements of d_{max} in the system dodecane – water under pulsation regimes with various intensity. He has also reported that the drops break mainly into two daughter drops. Consequently, the corresponding value of We_c is

$$\mathrm{We}_c = 0.26 \tag{A.7'}$$

The calculated data for d_{max} given in Table 1 within the text are obtained by using (Eq. (A.7')) and Eq. (17) in Eq. (16).

References

[1] Park, H., Ph.D. Thesis, INP, Toulouse, 1980.
[2] S.Dimitrova Al Khani, C. Gourdon, G. Casamatta, Chem. Eng. Sci. 44(6) (1989) 1295.
[3] J.F. Milot, J. Duhamet, C. Gourdon, G. Casamatta, Chem. Eng. J. 45 (1990) 111.
[4] Hanssens, A., in: Proc. Summer School Liq. Extr., Toulouse, 1991.
[5] Sukmanee, S., Ph.D. Thesis, INP, Toulouse, 1984.
[6] Srisuwan, G., Ph.D. Thesis, INP, Toulouse, 1988.
[7] Haunold, C., Ph.D. Thesis, INP, Toulouse, 1991.
[8] Schistel, R., Modélisation et simulation des écoulements turbulents, Traités des Nouvelles Technologies, Série Mecanique, Hermes, 1993.
[9] B.E. Launder, D.B. Spalding, Comp. Methods in Appl. Mech. Eng. 3 (1974) 269.
[10] G. Angelov, A. Line, C. Gourdon, Chem. Eng. J. 45 (1990) 87.
[11] J.P. Magnaud, D. Grand, M. Villand, Advances in Reactor Phys. Math. and Comp. 3 (1987) 1665.
[12] G. Angelov, C. Gourdon, Hung. J. Ind. Chem. 25 (1997) 223.
[13] Oh, W.Z., Ph.D. Thesis, INP, Toulouse, 1984.
[14] Laulan, A., Ph.D. Thesis, INP, Toulouse, 1980.
[15] Le Garrec, S., Ph.D. Thesis, 1992, CNAM, Paris.
[16] M. Aoun Nabli, P. Guiraud, C. Gourdon, Chem. Eng. Sci. 52(14) (1997) 2353.
[17] Hinze, J.O., Turbulence, McGraw-Hill, 1987.
[18] G. Narsimhan, J.P. Gupta, D. Ramkrishna, Chem. Eng. Sci. 34 (1979) 257.
[19] Gourdon, C., D.Sc. Thesis, INP, Toulouse, 1989.